Medbiotech Journal

MBTJ, 4(2): 57-61, 2020

Research Paper

Synthesis of Aniline through Palladium Nanoparticles over Alumina Catalyst

Husam Ali*, Jafar Arfa

Department of Chemistry, Baghdad University of Technology, Baghdad, Iraq

Received: 08 March 2020 Accepted: 15 May 2020 Published: 01 June 2020

Abstract

Aniline was synthesized by catalytic hydrogenation of nitrobenzene (NB) on nano-sized Pd on γ-Al_2O_3 catalyst prepared by sol-gel method. The catalyst was characterized by SEM and XRD. The average particle of Pd catalyst was 36 nm. In hydrogenation reaction of nitrobenzene, the hydrogenation rate was zero-order with respect to nitrobenzene and increased with increasing of hydrogen pressure. Compared with commercial Pd/γ-Al_2O_3, catalytic activity and selectivity of the as-prepared Pd/γ-Al_2O_3 is superior. The reason proposed for higher catalytic activity of nano-sized Pd is the small particle size and high-density surface defects.

Keywords: Nitrobenzene; Aniline; Nano-sized Pd on γ-Al_2O_3; Catalytic Hydrogenation

How to cite the article:
H. Ali, J. Arfa, Synthesis of Aniline through Palladium Nanoparticles over Alumina Catalyst, Medbiotech J. 2020; 4(2): 57-61, DOI: 10.22034/MBT.2020.109580.

1. Introduction

Aniline is a commercially important intermediate for the manufacturing of polyurethane (used in production of MDI, resin foams, automotive coating, shoe soles, spring components and rubber processing chemicals), herbicides, dyes and pigments, specialty fibers and drugs [1-3] . Aniline can be simply produced from benzene in two steps: First, benzene is nitrated (reacted with nitric acid) to yield nitrobenzene. Second, nitrobenzene is reduced to give aniline [4-6] . A variety of reducing agents are effective for the reduction, including hydrogen sulfide, iron, zinc, tin and hydrogen in presence of suitable catalysts such as Pd, Pt, Ni and etc. [7-9] .

Due to Some problems (such as long-time separation and potentially dangers) and the existing of BTX (Benzene, Toluene and Xylene) unit in petrochemical industry, it seems the catalytic hydrogenation is a preferred process in petrochemical industry [10-12] . Although using of palladium on activated carbon (Pd/C) leads to the highest yields in the three-phase process, however the problems such as separation and strength of the catalyst suggest that use of Pd/γ-Al_2O_3 which has the area less than carbon. It means the use of higher amount of Pd/γ-Al_2O_3 than Pd/C [13-15] .

In recent years, nanoparticles have received increasing attention since such metals exhibits a great many chemical and physical characteristics and potential technological applications. These are distinct both from those of the bulk phase and those from isolated atoms or molecules. Therefore, it may seem the use of nano-sized Pd on γ-Al_2O_3 enhances the reaction yield as Pd/C [16-18] .

In this research, it will be attempted to synthesize aniline from nitrobenzene over nano-sized Pd on γ-Al_2O_3 catalyst. The nano-sized Pd on γ-Al_2O_3 was prepared by sol-gel method. The textural properties of the nano-catalyst were characterized

*Corresponding author email: husam.ali@chemhitech.ir

by SEM and XRD. Attention is chiefly paid to the catalytic properties of nano-sized Pd on γ-Al_2O_3 in the synthesis of aniline from nitrobenzene, in comparison with Pd/γ-Al_2O_3 and Pd/C. At the same time, some reasons for better catalytic properties of nano-sized Pd on γ-Al_2O_3 are proposed.

2. Experimental

2.1. Catalyst preparation and characterization

In a typical preparation of nano sized Pd on γ-Al_2O_3 sample, aluminum tri-sec butoxide (ATB) was added to sec-butanol followed by thorough mixing. A second solution, consisting $H_2PdCl_4.xH_2O$ dissolved in warm acetone, was prepared. This Pd salt solution was added to the ATB-alcohol mixture and the solution was stirred thoroughly. A solution consisting of H_2O dissolved in methanol was added to the previous mixture containing ATB and the Pd salt. The resultant mixture was stirred at room temperature in a rotavapor. The sample was heated to 313 K and maintained at that temperature with continual stirring. The temperature was then reduced to 313 K and stirring continued for 1hr more. The sample was maintained at 333 K for 20hr with continuous stirring. The temperature was then raised to 353 K and maintained at that temperature for 1hr. Finally, the temperature was increased to 373 K and the solvent allowed to evaporate over a 30 min period. The sample was then dried in an oven at 393 K for 24 hr.

The dried sample was pretreated in a flow system using the following sequence of steps: The sample was heated in flowing He at the rate of 10 K/min to a final temperature of 773 K. Heating in He at a flow rate of 30cm^3/min was continued for 15 min at 773 K followed by heat treatment in O_2 at the same temperature for 2 hr and then in H_2 at 773 K for 3 hr. The H_2 was again replaced by He and the temperature increased to 793 K for 1hr. Finally, the sample was cooled to room temperature in flowing He. Portions of the pretreated samples were sent for ICP analysis in order to determine the actual Pd loading [1, 19, 20] .

XRD patterns were obtained on a Brucker D8 advance instrument with Pd-filtered CuKα radiation at 40kV and 30mA, employing a scanning rate of 0.05 s^{-1} in the 2θ range from 35 to 80°. The morphology was observed by SEM, LEO-1530VP. The mean particle size and size distribution of as-prepared Pd nanoparticles were measured by laser diffraction [17, 21, 22] .

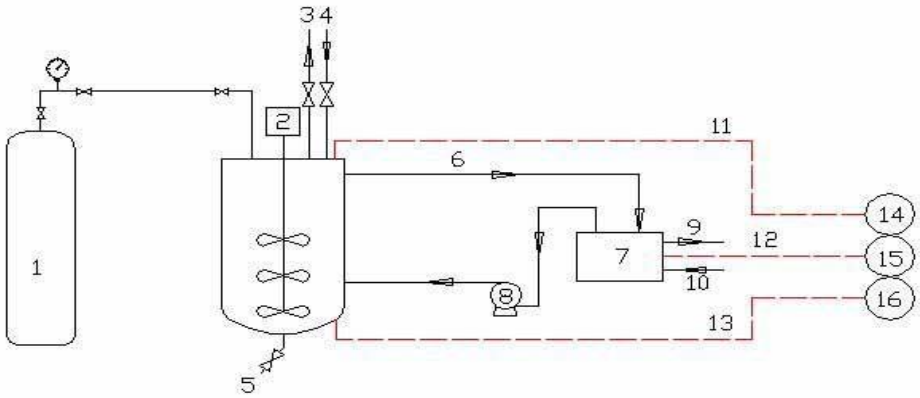

Figure 1. Experimental set up: 1-H_2 Cylinder, 2-Stirrer motor, 3-Vent, 4-Feed inlet, 5-Drainage and sampling, 6-Outlet cooled oil, 7-Oil bath, 8-Oil pump, 9-Outlet warmed water, 10-Inlet cooled water, 11-Reactor pressure signal, 12-Oil bath temperature signal, 13-Reactor temperature signal, 14-Reactor pressure recorder, 15-Oil bath temperature recorder, 16Reactor temperature recorder

2.2. Experimental set-up and procedure

The hydrogenation process was carried out in an isothermal 1L stainless steel autoclave (Buchi AG, Switzerland), which allows isothermal conditions due to a heating jacket (Fig.1). The hydrogen was supplied at the same rate that it was consumed under isobaric reaction conditions. The samples for the analysis were drawn via a sampling tube.

The experiments were carried out using the following procedure: First, nitrobenzene (Sigma Switzerland, 99%) was dissolved in a mixture of 91%wt of isopropanol (Fluka, 99%) and 9%wt distilled water. The reactor was filled with 300 mL solution and the solid catalyst (from 0.5 to 3 g) was added. Second, the reaction was initiated by removing the air from the reactor by purging with hydrogen and stirring the solution at 1500 rpm. The temperature was controlled at 323 K and the hydrogen partial pressure was kept constant between 3 and 14 bar. The samples were analyzed

by a gas chromatography (GC, Perkin Elmer- 8420) with product separation in a fused silica capillary column (30m, 0.53mmID) and a FID detector.

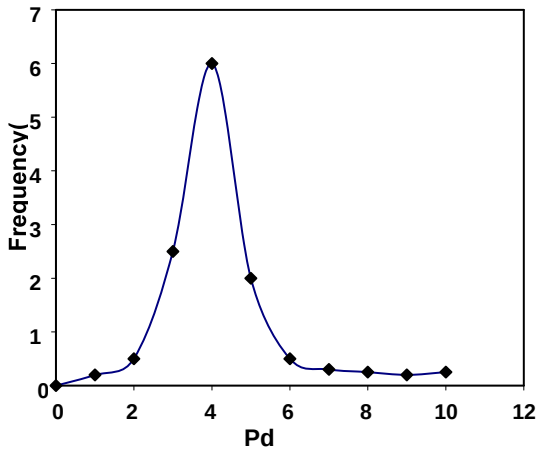

Figure 2. Size distribution of nano-sized Pd

2.3. Catalyst characterization

The average crystalline size was estimated by the Debye-Scherrer method to be in the range of 40nm from XRD data. The size distribution for nano-sized Pd measured by Mastersizer 2000 is shown in Figure 2. The result yields an average Pd particle size of 36 nm. The SEM micrograph of Pd nanoparticles is shown in Figure 3. Individual Pd particles are spherical in shape.

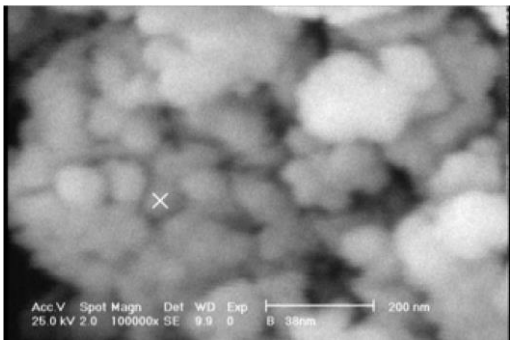

Figure 3. SEM image of nano-sized Pd particles in nano-sized Pd on γ-Al2O3

3. Results and discussion

The preliminary experiments on the hydrogenation of nitrobenzene indicated that no hydrogenation reaction occurred in the absence of the catalyst, which confirmed the absence of any noncatalytic reaction. Moreover, at a fixed temperature, the partial pressure of solvent isopropanol-water also remained constant. So, the decrease of the pressure in the reservoir vessel with time was caused only by catalytic hydrogenation of nitrobenzene to aniline. Therefore, in this manuscript catalytic activity could be expressed by hydrogenation rate defined as the amount of hydrogen consumed per minute and per gram of the nanocatalyst.

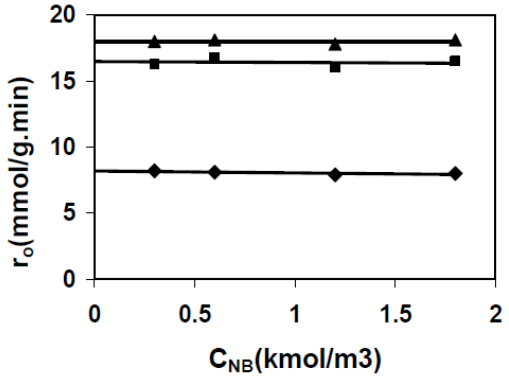

Figure 4. Effect of the concentration of nitrobenzene on initial rate. Reaction conditions: T=323 K, P=5 bar, stirring speed=1500rpm, -♦- $m_{Pd/\gamma\text{-}Al2O3}$=2.5 g/dm^3, -■- $m_{nano\text{-}Pd\ on\ \gamma Al2O3}$=0.8 g/dm^3, -▲-$m_{Pd/C}$=2.5 g/dm^3

The effects of nitrobenzene concentration and hydrogen pressure on the reaction rate were investigated in the presence of Pd/γ-Al_2O_3, nano- Pd on γ-Al_2O_3 and Pd/C; the results are shown in Figure 4 and 5. The effect of nitrobenzene concentration on the initial rate of hydrogenation (Figure 4) shows zero-order dependence at 0.25-1.8 kmol.m^{-3} concentrations. Compared with the concentration of the hydrogen dissolved in isopropanol aqueous solution, nitrobenzene concentration might be seemed to be a constant. Therefore, the reaction rate could not change with the variation of nitrobenzene concentration. A noticeable point is the lower activity of Pd/γ-Al_2O_3 than nano Pd on γ-Al_2O_3. The effect of hydrogenation partial pressure on the initial rate of hydrogenation was investigated at 323K in the pressure range of 3-14 bar (Figure 5). The hydrogenation rate increase with the increase of the hydrogen partial pressure. Also, it is seen more activity of nano- Pd on γ-Al_2O_3 than Pd/γ-Al_2O_3.

The catalytic activity comparison of the nano-sized Pd on γ-Al_2O_3 and Pd/C is shown in Figure 6. The hydrogenation rate on the nano-sized Pd/γ-Al_2O_3 is nearly the same as Pd/C at similar reaction conditions.

On the basis of similar reaction [22, 23] , it is suggested that the reason for higher catalytic activity of nano-sized Pd on γ-Al_2O_3 than Pd/γ-Al_2O_3 is a combination effect of the small particle size and the high density surface defects.

The product of hydrogenation reaction was analyzed and it was observed that in the reaction products catalyzed by the nano- Pd on γ-Al_2O_3, no other impurity existed.

An important and attractive point in Figures 4-6 is the less amount of nano- Pd on γ-Al_2O_3 than Pd/γ-Al_2O_3 and Pd/C, so that the amount of nano- Pd on

γ-Al_2O_3 is 1/3 of others (for simplicity, Pd loading in nano- Pd/γ-Al_2O_3 , Pd/γ-Al_2O_3 and Pd/C were taken 5% measured by ICP). In other words, nanosizing Pd particles leads to the higher speed in reaction and and less consumption of the as-prepared catalyst.

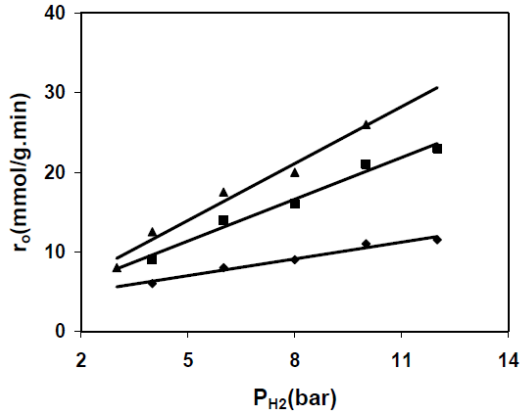

Figure 5. Effect of hydrogen partial pressure on initial rate. Reaction conditions: T=323 K, stirring speed=1500rpm, -♦- $m_{Pd/\gamma\text{-}Al2O3}$=2.5 g/$dm^3$, -■-$m_{nano\text{-}Pd\ on\ \gamma\text{-}Al2O3}$=0.8 g/$dm^3$, -▲-$m_{Pd/C}$=2.5 g/$dm^3$

4. Conclusions

In this work, aniline was synthesized by catalytic hydrogenation of nitrobenzene over as prepared nano-sized Pd in a laboratory autoclave. The following results were obtained:

1-The average particle size of the as-prepared Pd is 36nm.

2-The hydrogenation rate is zero-order dependent on nitrobenzene and increases with increasing of hydrogen pressure.

3-The activity and selectivity of the as-prepared Pd are superior compared with those of the conventional Pd/γ-Al_2O_3.

4- Also, nanosizing of Pd particles caused higher speed in reaction and less consumption of the as-prepared catalyst than conventional Pd/γ-Al_2O_3 and Pd/C.

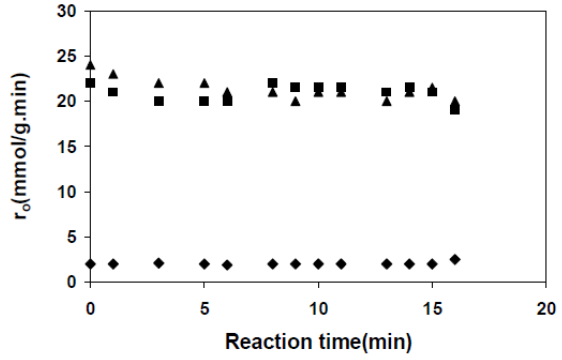

Figure 6. Correlation between catalytic activity of the catalysts. Reaction conditions: T=323 K, stirring speed=1500rpm, -♦- $m_{Pd/\gamma\text{-}Al2O3}$=2.5 g/$dm^3$, -■-$m_{nano\text{-}Pd\ on\ \gamma\text{-}Al2O3}$=0.8 g/$dm^3$, -▲-$m_{Pd/C}$=2.5 g/$dm^3$

References

1. Ryan SM, Mantovani G, Wang X, Haddleton DM, Brayden DJ. 2008. Advances in PEGylation of important biotech molecules: delivery aspects. *Expert Opinion on Drug Delivery* 5(4): 371-383.
2. Ghasemi E, Raofie F, Najafi NM. 2011. Application of response surface methodology and central composite design for the optimisation of supercritical fluid extraction of essential oils from Myrtus communis L. leaves. *Food Chemistry* 126(3): 1449-1453.
3. Ahmadi M, Vahabzadeh F, Bonakdarpour B, Mofarrah E, Mehranian M. 2005. Application of the central composite design and response surface methodology to the advanced treatment of olive oil processing wastewater using Fenton's peroxidation. *Journal of Hazardous Materials* 123(1): 187-195.
4. Santharaman P, Venkatesh KA, Vairamani K, Benjamin AR, Sethy NK, Bhargava K, et al. 2017. ARM-microcontroller based portable nitrite electrochemical analyzer using cytochrome c reductase biofunctionalized onto screen printed carbon electrode. *Biosensors and Bioelectronics* 90: 410-417.
5. Hwang J-Y, Shin US, Jang W-C, Hyun JK, Wall IB, Kim H-W. 2013. Biofunctionalized carbon nanotubes in neural regeneration: a mini-review. *Nanoscale* 5(2): 487-497.
6. Basak G, Hazra C, Sen R. 2020. Biofunctionalized nanomaterials for in situ clean-up of hydrocarbon contamination: A quantum jump in global bioremediation research. *Journal of Environmental Management* 256: 109913.
7. Kar S, Biswas S, Chaudhuri S. 2005. Catalytic growth and photoluminescence properties of ZnS nanowires. *Nanotechnology* 16(6): 737-740.
8. Jalali-Heravi M, Parastar H, Ebrahimi-Najafabadi H. 2009. Characterization of volatile components of Iranian saffron using factorial-based response surface modeling of ultrasonic extraction combined with gas chromatography–mass spectrometry analysis. *Journal of Chromatography A* 1216(33): 6088-6097.
9. Lewis LN. 1993. Chemical catalysis by colloids and clusters. *Chemical Reviews* 93(8): 2693-2730.
10. Kheirabadi MA, Jafari MH, Alizadeh F, Basiri Z, Oveisi K. 2019. Comparison and Satisfaction of Injured Management System for Students Athlete in the Sport Federations. *Journal of Computational and Theoretical Nanoscience* 16(1): 284-288.
11. Kheirabadi MA, Rahimi G, Zamani A, Alizadeh F, Basiri Z, Oveisi K. 2019. The comparison between the attitudes of employees and clients towards organizational intelligence (case study: Isfahan General Directorate of Sports and Youth). *Revista Latinoamericana de Hipertension* 14(1): 62-69.
12. Yamamoto T, Kishimoto S, Iida S. 2001. Control of valence states for ZnS by triple-codoping method.

Physica B-condensed Matter - PHYSICA B 308: 916-919.
13. Hu J, Bando Y, Zhan J, Golberg D. 2005. Growth of Wurtzite ZnS Micrometer-Sized Diskettes and Nanoribbon Arrays with Improved Luminescence. *Advanced Functional Materials* 15(5): 757-762.
14. Li LS, Pradhan N, Wang Y, Peng X. 2004. High Quality ZnSe and ZnS Nanocrystals Formed by Activating Zinc Carboxylate Precursors. *Nano Letters* 4(11): 2261-2264.
15. Jiang Y, Meng X-M, Liu J, Xie Z-Y, Lee C-S, Lee S-T. 2003. Hydrogen-Assisted Thermal Evaporation Synthesis of ZnS Nanoribbons on a Large Scale. *Advanced Materials* 15(4): 323-327.
16. Zhang H, Ji Y, Ma X, Xu J, Yang D. 2003. Long Bi2S3nanowires prepared by a simple hydrothermal method. *Nanotechnology* 14(9): 974-977.
17. Zhao Y, Zhang Y, Zhu H, Hadjipanayis GC, Xiao JQ. 2004. Low-Temperature Synthesis of Hexagonal (Wurtzite) ZnS Nanocrystals. *Journal of the American Chemical Society* 126(22): 6874-6875.
18. Kheirabadi MA, Jafari MH, Alizadeh F, Basiri Z, Oveisi K. 2019. Making an entity-relationship model of the knowledge management process with strategic thinking. *Revista Latinoamericana de Hipertension* 14(1): 55-61.
19. Velikov KP, van Blaaderen A. 2001. Synthesis and Characterization of Monodisperse Core−Shell Colloidal Spheres of Zinc Sulfide and Silica. *Langmuir* 17(16): 4779-4786.
20. Lakshmi PVB, Raj KS, Ramachandran K. 2009. Synthesis and characterization of nano ZnS doped with Mn. *Crystal Research and Technology* 44(2): 153-158.
21. Li Y, Li X, Yang C, Li Y. 2004. Ligand-Controlling Synthesis and Ordered Assembly of ZnS Nanorods and Nanodots. *The Journal of Physical Chemistry B* 108(41): 16002-16011.
22. Dhas NA, Zaban A, Gedanken A. 1999. Surface Synthesis of Zinc Sulfide Nanoparticles on Silica Microspheres: Sonochemical Preparation, Characterization, and Optical Properties. *Chemistry of Materials* 11(3): 806-813.
23. Wang Z, Daemen LL, Zhao Y, Zha CS, Downs RT, Wang X, et al. 2005. Morphology-tuned wurtzite-type ZnS nanobelts. *Nature Materials* 4(12): 922-927.